Inorganic Chemistry
Article

Inorg. Chem. **2009**, *48*, 9737–9741 **9737**
DOI: 10.1021/ic901324n

Structural Phase Transformations of Mg_3N_2 at High Pressure: Experimental and Theoretical Studies

Jian Hao,[†] Yinwei Li,[†] Qiang Zhou,[†] Dan liu,[†] Min Li,[†] Fangfei Li,[†] Weiwei Lei,[†] Xiaohui Chen,[†] Yanming Ma,[†] Qiliang Cui,*[,†] Guangtian Zou,[†] Jing Liu,[‡] and Xiaodong Li[‡]

[†]*State Key Laboratory of Superhard Materials, Jilin University, Changchun 130012, People's Republic of China, and* [‡]*Beijing Synchrotron Radiation Laboratory, Institute of High Energy Physics, Chinese Academy of Sciences, Beijing 100039, People's Republic of China*

Received July 9, 2009

The structural behavior of Mg_3N_2 has been investigated up to 40.7 GPa at room temperature by means of angle-dispersive X-ray diffraction. A reversible, first-order structural phase transition from the ambient cubic phase ($Ia\bar{3}$) to a high-pressure monoclinic phase ($C2/m$) is found to start at ~20.6 GPa and complete at ~32.5 GPa for the first time. The equation of state determined from our experiments yields bulk moduli of 110.7(2) and 171.5(1) GPa for the cubic and monoclinic phases, respectively, indicating higher incompressibility of the high-pressure phase of Mg_3N_2. First-principles calculations reproduced the phase stability and transition pressure determined in our experiment. In addition, a second phase transition from the monoclinic phase to a hexagonal phase ($P\bar{3}m_1$) was predicted around 67 GPa for Mg_3N_2. The electronic band structures of three phases of Mg_3N_2 are also calculated and discussed.

Introduction

Solid nitride materials have become a rapidly growing field of interest in recent years.[1,2] Some binary nitrides, such as AlN and Si_3N_4, have been widely used as high-performance engineering and substrate materials in the semiconductor industry.[1] Magnesium nitride, Mg_3N_2, is a salt-like nitride[3] and is well-known for its role as a nitriding agent for the practical preparation of various nitrides such as rare-earth nitrides,[3] $MgSiN_2$,[4,5] and AlN.[6] Mg_3N_2 also possesses catalytic properties, which are useful in the synthesis of superhard silicon nitride and cubic boron nitride.[7,8]

Under ambient conditions, Mg_3N_2 crystallizes in the cubic antibixbyite (anti-C-type, space group $Ia\bar{3}$) structure of the mineral $(Mn,Fe)_2O_3$ known also for other group II metal nitrides M_3N_2 (M = Be, Ca, Zn, Cd).[9−12] The cubic bixbyite (C-type) structure has been considered as the type structure and has been carefully refined for many sesquioxides such as Sc_2O_3,[13] Y_2O_3,[14] Er_2O_3,[15] Gd_2O_3,[16] In_2O_3,[17] and so on. The structural behavior of these cubic bixbyite materials under high pressures has been the topic issue of research in recent years. Interestingly, sesquioxides present different phase sequences at high pressures and/or high temperatures. Most sesquioxides usually follow the sequence of C → B (monoclinic, space group $C2/m$) → A (hexagonal, space group $P\bar{3}m_1$) at high pressures and/or high temperatures.[15,18−20] However, different phase sequences have been reported in some C-type sesquioxides. It is verified that Gd_2O_3 transforms directly to the A-type structure at high pressure[16] and In_2O_3 transforms to the corundum (hexagonal, space group

*To whom correspondence should be addressed. E-mail: cql@jlu.edu.cn.

(1) Niewa, R.; DiSalvo, F. *Chem. Mater.* **1998**, *10*, 2733.
(2) Metselaar, R. *Pure Appl. Chem.* **1994**, *66*, 1815.
(3) Parkin, I. P.; Nartowski, A. M. *Polyhedron* **1998**, *17*, 2617.
(4) Groen, W. *J. Eur. Ceram. Soc.* **1993**, *12*, 413.
(5) Bruls, R. J.; Hintzen, H. T.; Metselaar, R. *J. Mater. Sci.* **1999**, *34*, 4519.
(6) Kobashi, M.; Okayama, N.; Choh, T. *Mater. Trans., JIM* **1997**, *38*, 260.
(7) Lorenz, H.; Peun, T.; Orgzall, I. *Appl. Phys. A: Mater. Sci. Process.* **1997**, *65*, 487.
(8) Lorenz, H.; Kühne, U.; Hohlfeld, C.; Flegel, K. *J. Mater. Sci. Lett.* **1988**, *7*, 23.
(9) Stackelburg, M. V.; Paululus, R. *Z. Phys. Chem. B* **1933**, *B22*, 305.
(10) Partin, D. E.; Williams, D. J.; O'Keeffe, M. *J. Solid State Chem.* **1997**, *132*, 56.
(11) Juza, R.; Hahn, H. *Z. Anorg. Allg. Chem.* **1940**, *244*, 125.
(12) Paszkowicz, W.; Knapp, M.; Domagala, J. Z.; Kamler, G.; Podsiadlo, S. *J. Alloys Compd.* **2001**, *328*, 272.
(13) Schleid, T.; Meyer, G. *J. Less-Common Met.* **1989**, *149*, 73.
(14) Antic, B.; Oennerud, P.; Rodic, D.; Tellgren, R. *Powder Diffr.* **1993**, *8*, 216.
(15) Guo, Q.; Zhao, Y.; Jiang, C.; Mao, W. L.; Wang, Z.; Zhang, J.; Wang, Y. *Inorg. Chem.* **2007**, *46*, 6164.
(16) Zhang, F. X.; Lang, M.; Wang, J. W.; Becker, U.; Ewing, R. C. *Phys. Rev. B* **2008**, *78*, 064114.
(17) Yusa, H.; Tsuchiya, T.; Sata, N.; Ohishi, Y. *Phys. Rev. B* **2008**, *77*, 064107.
(18) Hoekstra, H. R.; Gingerich, K. A. *Science* **1964**, *146*, 1163.
(19) Bartos, A.; Lieb, K. P.; Uhrmacher, M.; Wiarda, D. *Acta Crystallogr. B* **1993**, *49*, 165.
(20) Aldebert, P.; Traverse, J. P. *Mater. Res. Bull.* **1978**, *14*, 303.

Published on Web 09/15/2009

$R\bar{3}c$) structure[21−24] and then to the Rh_2O_3 (II)-type (orthorhombic, space group *Pbna*) structure under high pressure and temperature.[17] Surprisingly, there has been no report on what phases the corresponding anti-C-type compounds will adopt under pressure. Therefore, the pressure-induced phase sequence of the anti-C-type Mg_3N_2 is motivated in relation to the high-pressure transitions in C-type sesquioxides.

Here, we report the outcome of a high-pressure study on anti-C-type Mg_3N_2 up to 40.7 GPa at room temperature using in situ angle-dispersive X-ray diffraction (ADXD) measurement. A high-pressure phase with the monoclinic $C2/m$ (anti-B-type) structure was observed for the first time in Mg_3N_2 at pressures higher than 20.6 GPa. In addition, our theoretical results predicted that there is a second phase transition from the anti-B-type to the hexagonal $P\bar{3}m_1$ (anti-A-type) structure at about 67 GPa.

Experimental and Computational Details

Commercially available Mg_3N_2 powder (Alfa Products, purity of 99.6%) was loaded into a gasketed high-pressure Mao−Bell-type diamond anvil cell with 400 μm culet diamond anvils. A 120-μm-diameter hole was drilled through the center of a preindented 60-μm-thick T-301 stainless steel gasket to form a sample chamber. Mg_3N_2 is extremely sensitive to moisture and readily hydrolyzes with common pressure-transmitting media. In order to restrain such hydrolyzation, silicone grease was used as the pressure-transmitting media. The pressure was determined from the frequency shift of the ruby R_1 fluorescence line.[25]

ADXD experiments were carried out up to 40.7 GPa at room temperature using a synchrotron X-ray source (λ = 0.6199 Å) of the 4W2 High-Pressure Station of Beijing Synchrotron Radiation Facility (BSRF). The diffraction data were collected using MAR165 CCD detector. The Bragg diffraction rings were recorded with an imaging plate detector, and the two-dimensional X-ray diffraction (XRD) images were analyzed using the *FIT2D* software, yielding one-dimensional intensity versus diffraction angle 2θ patterns.[26] The average acquisition time was 300 s. The sample−detector distance and geometric parameters were calibrated using a CeO_2 standard from NIST. High-pressure synchrotron XRD patterns were fitted by Rietveld profile matching using the *MATERIAL STUDIO* program. Unit cell parameters were obtained using the *DICVOL91* program. During each refinement cycle, the scale factor, background parameter, and cell parameter were optimized.

First-principles calculations were carried out using the plane-wave pseudopotential method within the framework of density functional theory (DFT) with the VASP code.[27] The generalized gradient approximation (GGA)[28] exchange-correlation functional was employed. The all-electron projector-augmented wave method[29] was adopted with a same plane-wave kinetic energy cutoff of 520 eV for all possible Mg_3N_2 phases. The use of Monkhorst−Pack k-point meshes of $4 \times 4 \times 4$, $6 \times 6 \times 3$, $14 \times 14 \times 8$, and $6 \times 6 \times 6$ for anti-C-type, anti-B-type, anti-A-type, and anticorundum structures, respectively, was shown to give excellent convergence of the total energies, energy differences, and structural parameters at both ambient and high pressures.

Results and Discussion

The schematic ambient crystal structure of the cubic anti-C-type Mg_3N_2 is shown in Figure 1a. In this structure, Mg and two inequivalent N (labled as N1 and N2) atoms occupy Wyckoff 48*e*, 24*d*, and 8*b* positions, respectively. The Mg atoms are in tetrahedra sites of an approximately cubic close-packed array of N atoms. Each N1 has four shorter and two longer bond distances with Mg, while N2 is octahedrally coordinated with six Mg atoms, forming a Mg_6N polyhedron. The selected XRD patterns of Mg_3N_2 with increasing pressure are shown in Figure 2. The Rietveld refinement of Mg_3N_2 performed at 1.5 GPa (Figure 3a) shows a good agreement with the ambient cubic structure with a lattice constant of 9.936(7) Å. During compression, all diffraction peaks shift toward higher 2θ angles. However, no shape change is observed below 20.6 GPa, indicating that the sample remained as the anti-C-type.

Above 20.6 GPa, it is observed that the relative intensity of the five main peaks (2,1,1), (2,2,2), (4,0,0), (3,3,2), and (4,4,0) of the anti-C-type Mg_3N_2 decreases with increasing pressure. At the same time, two new diffraction peaks marked with asterisks begin to appear in the XRD patterns at 20.6 GPa. These results indicate that a pressure-induced phase transformation occurred at 20.6 GPa. However, the peaks of the anti-C-type Mg_3N_2 persist until 32.5 GPa. These peaks completely disappear, and the sample is fully converted to the new phase up to nearly 32.5 GPa. The large pressure coexistence region (20.6−32.5 GPa) of two phases may be partially due to the nonhydrostatic stresses created by using the grease oil as a pressure medium.[30] Figure 3b presents the Rietveld refinement of Mg_3N_2 performed at 32.5 GPa, showing good agreement with a monoclinic cell with space group $C2/m$ with lattice parameters a = 12.229(9) Å, b = 3.157(9) Å, c = 7.618(5) Å, and β = 99.03(9)°. In this structure, there are five Mg and three N sites in a unit cell, of which four Mg and three N atoms occupy the 4*i* (x, 0, z) position while the other Mg atom takes the 2*b* (0, 0.5, 0) position. The corresponding atomic positions at 32.5 GPa are listed in Table 1. It is found that the $C2/m$ structure is isostructural with the high-pressure B-type structure observed in bixbyite sesquioxides[15,18−20] but with an interchange of the cation and anion; we thus call this phase anti-B-type. As shown in Figure 1b, anti-B-type structure is a layer type with all atom sites at y = 0 or $^1/_2$. In each plane, corrugated sheets of Mg atoms alternating with similarly corrugated sheets of N atoms along the c axis are found. Each N atom is coordinated by seven Mg atoms, forming a Mg_7N polyhedron. The coordination of N1 and N2 is a distortion trigonal prism with six Mg atoms, while the seventh Mg−N bond is along the normal to a prism face. In addition, the coordination about the N3 atoms can be formally described as a distorted octahedron. However, the seventh Mg atom is almost too far away to be included in the primary coordination shell. With the pressure increasing, no further discontinuous change is observed in the XRD profiles up to 40.7 GPa.

(21) Remeika, J. P.; Marezio, M. *Appl. Phys. Lett.* **1966**, *8*, 87.
(22) Marezio, M.; Remeika, J. P. *J. Chem. Phys.* **1967**, *46*, 1862.
(23) Shannon, R. *Solid State Commun.* **1966**, *4*, 629.
(24) Prewitt, C. T.; Shannon, R. D.; Rogers, D. B.; Sleight, A. W. *Inorg. Chem.* **1969**, *8*, 1985.
(25) Mao, H. K.; Xu, J.; Bell, P. M. *J. Geophys. Res.* **1986**, *91*, 4673.
(26) Hammersley, A. P.; Svensson, S. O.; Hanfland, M.; Fitch, A. N.; Hausermann, D. *High Pressure Res.* **1996**, *14*, 235.
(27) Kresse, G.; Furthmüller, J. *Phys. Rev. B* **1996**, *54*, 11169.
(28) Perdew, J. P.; Burke, K.; Ernzerhof, M. *Phys. Rev. Lett.* **1996**, *77*, 3865.
(29) Blöchl, P. E. *Phys. Rev. B* **1994**, *50*, 17953.
(30) Hao, J.; Zou, B.; Zhu, P.; Gao, C.; Li, Y.; Liu, D.; Wang, K.; Lei, W.; Cui, Q.; Zou, G. *Solid State Commun.* **2009**, *149*, 689.

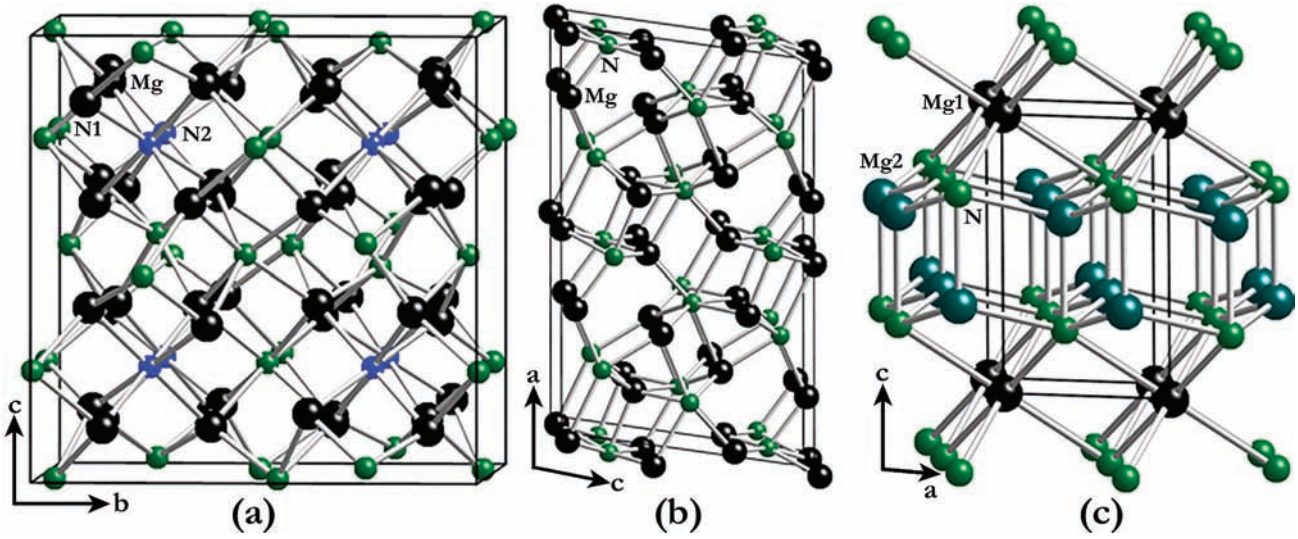

Figure 1. Schematic crystal structures of Mg_3N_2 polymorphs: (a) anti-C-type; (b) anti-B-type; (c) anti-A-type. The lattice parameters of the predicted high-pressure anti-A-type structure at 70 GPa are $a = b = 3.1767$ Å, $c = 4.7844$ Å, with atoms at Wyckoff positions 1*a* (Mg) (0, 0, 0), 2*d* (Mg) ($^1/_3$, $^2/_3$, 0.661), and 2*d* (N) ($^1/_3$, $^2/_3$, 0.231).

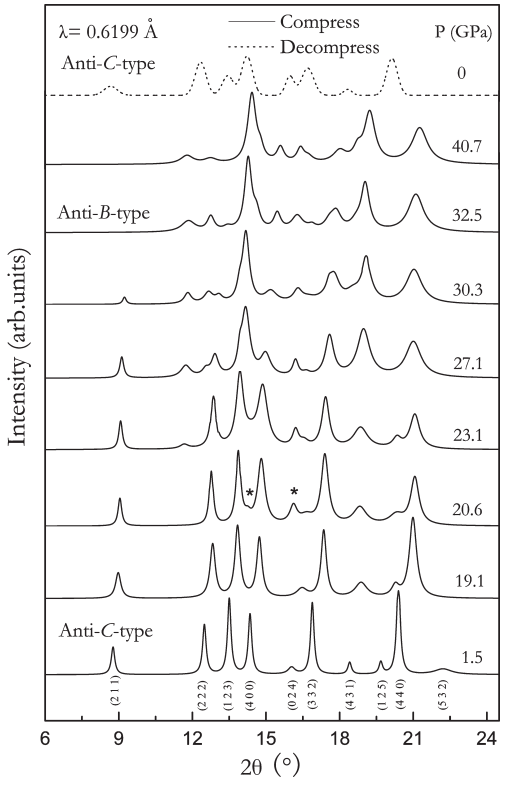

Figure 2. Selected XRD patterns of Mg_3N_2 with increasing pressure up to 40.7 GPa and then decompression to ambient pressure (from bottom to top) at room temperature. Asterisks marked in the profile at 20.6 GPa represent the peaks of the new phase. A pressure-induced structural transition is observed around 20.6 GPa and completed at 32.5 GPa.

The high-pressure anti-B-type phase of Mg_3N_2 is reversible and transforms back to the ambient phase during decompression back to zero pressure (Figure 2), indicating that the anti-C → anti-B phase transition is fully reversible. The refinement of the XRD pattern at room condition of Mg_3N_2 after decompression gives a lattice constant of 9.970(3) Å, which is in good agreement with the literature values.[10,12]

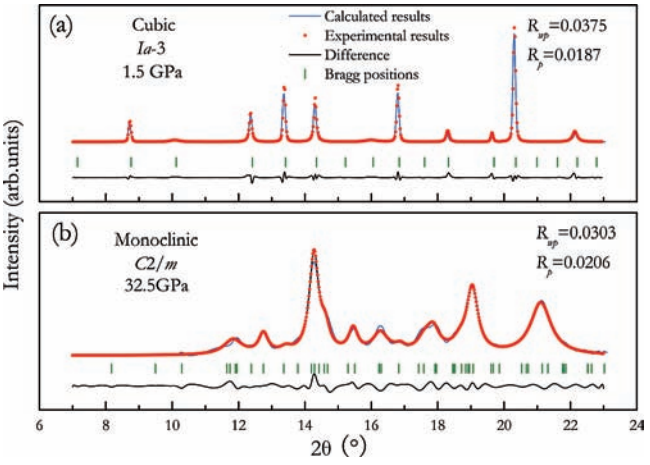

Figure 3. Rietveld refinement of the XRD patterns of Mg_3N_2 taken at 1.5 and 32.5 GPa: (a) structural refinement of the ambient cubic structure with space group of $Ia\bar{3}$; (b) structural refinement of the high-pressure monoclinic phase in the anti-B-type structure with space group *C*2/*m*.

Table 1. Atomic Coordinates and Isotropic Displacement Factors U_{iso} (Å^2) of the Monoclinic Anti-B-Type Structure for Mg_3N_2 at 32.5 GPa

atom	position	*x*	*y*	*z*	U_{iso}
Mg1	4*i*	0.827(6)	0	0.031(4)	0.0019(6)
Mg2	4*i*	0.795(1)	0	0.372(1)	0.0077(6)
Mg3	4*i*	0.127(8)	0	0.285(6)	0.0050(9)
Mg4	4*i*	0.469(1)	0	0.339(6)	0.0090(5)
Mg5	2*b*	0	0.5	0	0.0025
N1	4*i*	0.636(1)	0	0.484(2)	0.0037(4)
N2	4*i*	0.686(4)	0	0.136(9)	0.0023(7)
N3	4*i*	0.967(1)	0	0.184(5)	0.0075(6)

The normalized lattice parameters of the anti-C- and anti-B-type phases from the refinement as a function of the pressure are presented in Figure 4a. For comparison, our first-principles calculated results are also presented. One observes that the theory and experiment are in excellent mutual agreement. All lattice parameters in two phases decrease monotonically with increasing pressure, and the compressibilities of the *a*, *b*, and *c* axes in the anti-B-type

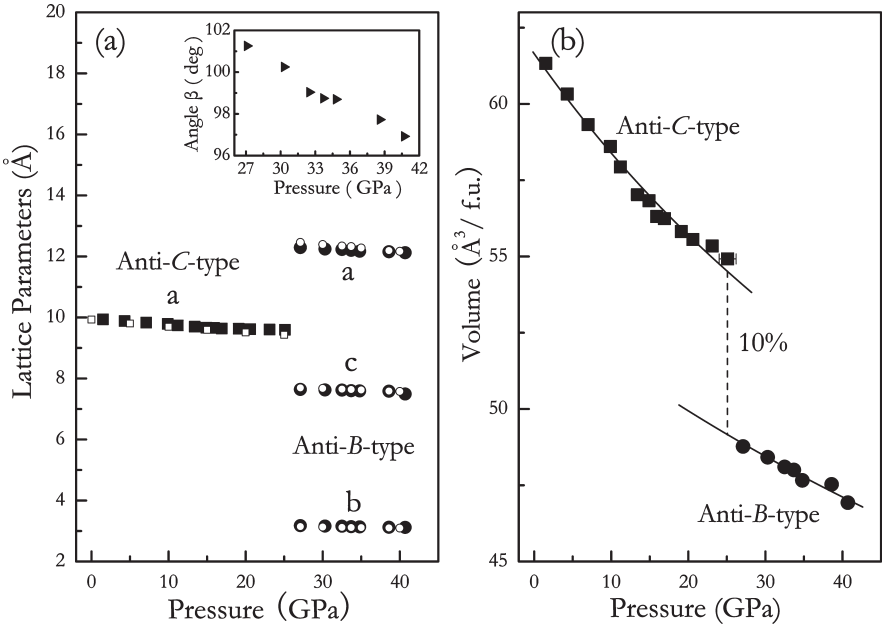

Figure 4. Pressure dependence of the lattice parameters (a) and cell volumes per formula unit (b) of the anti-C- and anti-B-type structures of Mg_3N_2. Solid and open symbols in part a represent experimental and theoretical results, respectively. The inset in part a is the β angle of the anti-B-type phase as a function of the pressure. Solid lines in part b are the fittings with BM EOSs.

structure are very close, suggesting that the high-pressure phase of Mg_3N_2 is isotropy. The pressure dependence of the volumes per Mg_3N_2 formula unit (fu) for the anti-C- and anti-B-type structures is shown in Figure 4b. There is about 10% volume shrinkage during the phase transition at ~25 GPa, indicating the first-order nature of the phase transition. The experimental pressure−volume data for the anti-C- and anti-B-type phases of Mg_3N_2 were fitted to a third-order Birch−Murnaghan (BM) equation of state (EOS)[31]

$$P = 1.5B_0[(V/V_0)^{-7/3} - (V/V_0)^{-5/3}]$$
$$[1+0.75(B_0' - 4)[(V/V_0)^{-3/2} - 1)]$$

where V_0 is the volume per formula unit at ambient pressure, with V being the volume per formula unit at pressure P given in GPa, B_0 is the isothermal bulk modulus, and B_0' is the first pressure derivative of the bulk modulus. With B_0' fixed at 4, we yield B_0 and V_0 of 110.7(2) GPa and 61.7(1) Å^3 for the anti-C-type phase and 171.5(1) GPa and 53.0(9) Å^3 for the anti-B-type phase, respectively. The large values of bulk moduli suggest that Mg_3N_2 is a high-incompressibility material. It is interesting to note that the bulk modulus of the high-pressure phase increases ~55% compared to that at the ambient-pressure phase, indicating an increasing incompressibility of Mg_3N_2 at extreme conditions.

The current XRD experiments revealed that Mg_3N_2 follows a phase sequence of anti-C → anti-B under pressure, which is consistent with most sesquioxides adopting a C → B phase transition. In order to confirm the transition pressure of the anti-C → anti-B transition for Mg_3N_2, a detailed first-principles calculation was performed. In addition to the anti-C- and anti-B-type structures, two hexagonal structures derived from the A-type and corundum structures of sesquioxides by interchanging the cations and anions were also considered to predict the possible post-anti-B-type phase for

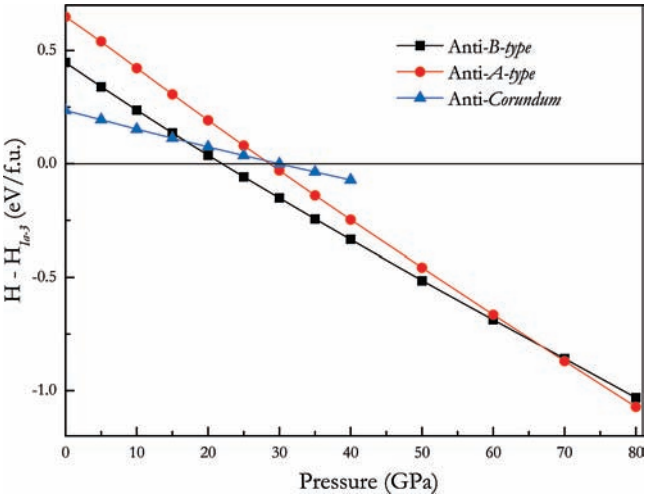

Figure 5. Calculated static enthalpies of the anti-B-type and two other considered anti-A-type and anticorundum structures with respect to the ambient anti-C-type structure as a function of the pressure.

Mg_3N_2. We denoted these two hexagonal structures as anti-A and anticorundum. The static enthalpies (T = 0 K) of different phases relative to that of the anti-C-type as a function of the pressure are plotted in Figure 5. It is obvious that the anti-C-type structure transforms to the anti-B-type structure at ~22 GPa. The value 22 GPa falls between the transition pressure ranges of 20.6−32.5 GPa observed in our X-ray experiments. Moreover, our results predict that the anti-A-type structure (Figure 1c) should also exist in Mg_3N_2 above 67 GPa. The stable field of the predicted anti-A-type polymorph is within reach of the current experimental techniques, and further experiments are necessary to investigate this high-pressure phase. The calculation rules out the existence of an anticorundum structure by the relatively higher enthalpy at all pressures. The phase sequence of anti-C → anti-B → anti-A for Mg_3N_2 is similar to the sequence found in most sesquioxides.[11−13] Other

(31) Birch, F. *J. Appl. Phys.* **1938**, *9*, 279.

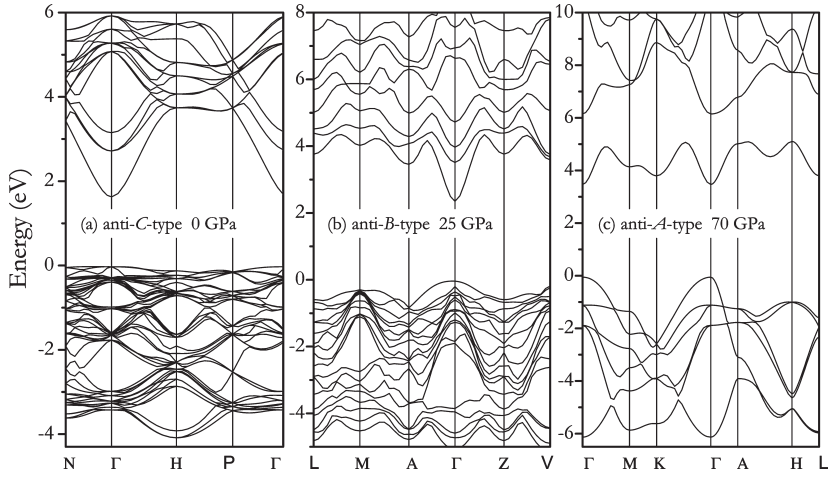

Figure 6. Calculated electronic band structures of Mg_3N_2 with (a) the anti-C-type structure at ambient pressure, (b) the anti-B-type structure at 25 GPa, and (c) the anti-A-type structure at 70 GPa.

group II metal nitrides (Ca_3N_2, Zn_3N_2, and Cd_3N_2) possess the same equilibrium structure as Mg_3N_2. Therefore, we suggest that these nitrides may adopt the same phase transitions as Mg_3N_2 at high pressures. However, in view of the different phase sequences found in the C-type sesquioxides,[11−19] future experimental effort is thus in great demand.

Electronic band structures for the three phases of Mg_3N_2 were calculated and presented in Figure 6. These suggest that all three phases of Mg_3N_2 are semiconducting because of the existence of direct band gaps at the Γ point. The calculated band gap of the anti-C-type Mg_3N_2 is 1.65 eV at ambient pressure, in agreement with the earlier theoretical results (1.63 and 1.85 eV),[32] whereas it is only about 59% of the measured value (2.8 eV[33]). The discrepancy between the theory and experiment is typical of the calculation method that we used, in which DFT-GGA calculations systematically underestimate the band gap in semiconductors and insulators (in most cases just 50−80% of the experimentally observed band gap). With increasing pressure, the band gap increases to 2.35 eV in the anti-B-type structure at 25 GPa and 3.48 eV in the anti-A-type structure at 70 GPa, as shown in Figure 6b,c.

(32) Orhan, E.; Jobic, S.; Brec, R.; Marchand, R.; Saillard, J. Y. *J. Mater. Chem.* **2002**, *12*, 2475.
(33) Fang, C. M.; De Groot, R. A.; Bruls, R. J.; Hintzen, H. T. *J. Phys.: Condens. Matter* **1999**, *11*, 4833.

Conclusions

In conclusion, a reversible phase transition from the ambient anti-C-type structure to a monoclinic structure has been unambiguously identified around 20.6 GPa and completed at 32.5 GPa based on synchrotron XRD. The refinement results suggest that the monoclinic phase is structurally identical with the anti-B-type ($C2/m$) structure. The observed phase stability and transition pressure are well explained by first-principles calculations. A second phase transition from the anti-B-type structure to the anti-A-type structure was predicted for Mg_3N_2 at 67 GPa by enthalpy calculations. Electronic band structure calculations show that the band gap increases with increasing pressure, suggesting the potential optical application of Mg_3N_2 at high pressures.

Acknowledgment. The authors are grateful to Yanchun Li and Xiaodong Li for their help during the experiments. XRD experiments of this work were performed at the 4W2 High-Pressure Station; BSRF assisted in the synchrotron measurement. High-Pressure Station is supported by the Chinese Academy of Sciences (Grants KJCX2-SW-N20 and KJCX2-SW-N03). This work was financially supported by the NSFC (50772043), the National Basic Research Program of China (Grants 2001CB711201 and 2005CB724400), and the Graduate Innovative Fund of Jilin University (Grants 20092003, 20091011, and MS20080217).